Chemistry Research Journal, 2018, 3(3):100-108

Available online www.chemrj.org

Research Article

ISSN: 2455-8990
CODEN(USA): CRJHA5

Hydrothermal Synthesis and Photoluminescence Property of Inorganic-Organic Nanohybrid Compound Based on Ni (II), MoO_3 and 4,4′- Bipyridine

Roya Ranjineh Khojasteh*, Fereshteh Hossein Pooly

Department of Inorganic Chemistry, Faculty of Chemistry, Tehran North Branch, Islamic Azad University, Tehran, Iran

Abstract A new nanocrystalline compound has been synthesized via hydrothermal method using $NiCl_2$ and MoO_3 and 4,4′-bipy (4,4′- bipyridine). The structure, morphology and photoluminescence property have been studied by using different analysis including X-ray Diffraction (XRD), Fourier Transform Infra Red (FT-IR) spectroscopy, Scanning Electron Microscopy (SEM), Photoluminescence (PL) spectra, Thermogravimetric Analysis (TGA-DTA) and Energy Dispersive X-ray spectroscopy (EDX). To fabricate the compound, the effect of different conditions, such as the concentration of initial reactants, pH values, temperature and reaction time, on structure and morphology of nanocrystals have been investigated. According to obtained results, the pH value influences the size of fabricated nanocrystals, the crystals size increased and nanostructures morphology changed with the increment in pH value. The results show, neutral or low alkaline conditions of pH are more favorable for formation of the nanocrystals. The prepared nanocrystal exhibit a strong PL peak at 453 nm at room temperature when excited by 270 nm wavelength. TGA and DTA analysis display a total weight loss of 10.73 %.

Keywords Hydrothermal, Nanohybrid, Nanocrystal, Ni, MoO_3, Bipyridine

Introduction

Due to observed unique properties of inorganic-organic nanohybrids in various industries, there is an increasing interest to fabricate and study these materials for different applications. It should be noticed that inorganic-organic nanohybrids display significant changes at nanoscale because of surface and volume properties as well as high surface-to-volume ratio [1-5].

Engineering of nanocrystals of inorganic-organic hybrid materials absorbs attention due to two important reasons including: (1) difference in their structural flexibility [6], (2) their capability to be used as catalyst, ion exchange, photochemistry, gas storage and electromagnetism [7-15]. Hydrothermal crystallization in the presence of multifunctional organic amines is one the methods utilized for the synthesis of these materials. Multifunctional nitrogenated organic ligands, such as *p*-phenylenediamine (ppda) [15-17], ethylenediamine (en) [19-20], 1, 10-phenanthroline (phen) [21-22] etc, are widely used in the structure of inorganic-organic nanohybrids owing to the fact that these ligands can act as structure-directing between molybdate building blocks to ease the formation of different networks. These ligands not only can be used as coordination factors to transition metals but also cause the formation of 1D or multi-dimensional networks by forming intermolecular interactions, such as hydrogen bonding [23-26]. These compounds are usually synthesized in solid state at temperature above 150 $^{\circ}$C. The advantage of this

method is the controlling of chemical homogeneity, purity, morphology, shape and phase of crystals under moderate conditions and, as a result, structural nanocrystals with various capabilities, like electronic properties, are obtained.
The crystalline structure of inorganic-organic hybrid materials of Mo and 4,4′- bipy has been mostly investigated [27-29]; however, the preparation of their nanoparticles has not been reported. Thus, we were interested in synthesizing these nanoparticles and studying their structure and properties. In this regard, we synthesized these nanoparticles and studied their structure and properties. In this paper, nanostructure powders of $NiCl_2$ and MoO_3 with 4,4′- bipy spacer group synthesized by hydrothermal method. The effect of different factors on hydrothermal process and the effect of pH values on the morphology of nanocrystals as well as their PL characteristic are investigated.

Materials and Methods

All starting materials were purchased from Aldrich and Merck and used without further purification. Powder X-ray Diffraction (PXRD) spectra were measured on a STOE-STADIP. Fourier Transform Infra Red (FT-IR) was recorded in KBr discs on a Perkin-Elmer 78 spectrophotometer. Scanning Electron Microscopy (SEM) and Energy Dispersive X-ray spectroscopy (EDX) were observed with EM 3200-KYKY. Photoluminescence (PL) spectra were performed with a Perkin Elmer LS55 spectrometer using a 150W xenon lamp as excitation source. Thermogravimetric Analysis (TGA-DTA) was performed on a BAHR STA 503 Thermal analyzer in air with a heating rate of 5 $^{\circ}$C/min.

General method to prepare nanocrystals

A mixture of $NiCl_2.6H_2O$ (0.024 g, 0.101 mmol), MoO_3 (0.014 g, 0.104 mmol), 4,4′-biyp (4,4′- bipyridine) (0.016 g, 0.102 mmol) and distilled water (10 g, 555.5 mmol) with mole ratios of 1:1:1:5555 (and repeat with 2:1:1:5555) stirred for 30 minutes at room temperature. The pH value of the suspension was precisely fixed at 2, 4, 6, 8 and 10 by using aqueous solutions of HCl and NaOH (1M). Then the suspension was transferred to a Teflon-lined stainless steel autoclave (25 mL) and heated to 200 $^{\circ}$C at the rate of 5 $^{\circ}$C/10 min. After 4 days, the temperature was decreased to the room temperature at the rate of 5 $^{\circ}$C/10 min. At the ending of the reaction, the pH value of the solution did not change. The filtered black precipitate was washed with distilled water and dried at room temperature in a desiccator. The obtained compound has a melting point of 1700 $^{\circ}$C and is insoluble in water and other common solvents.

Results and Discussion

Synthesis

Different factors influence the formation of nanocrystalline products. These factors are: the initial reactants type, molar ratio, pH value, reaction time and temperature during hydrothermal synthesis. By changing these factors, many reactions are performed under different conditions. Temperature and reaction time in the range of 150-200 $^{\circ}$C and 2-6 days are examined, respectively. Finally, we resulted that suitable nanocrystals are formed at 200 $^{\circ}$C after 4 days. No nanocrystalline products are formed when the initial reactant was changed from molybdenum trioxide to ammonium heptamolybdate tetrahydrate.

Powder X-ray diffraction

PXRD analysis is applied to investigate the phase-structural changes of nanocrystals. On the basis of XRD data, it is observed that synthesized nanocrystals from initial reactants with molar ratio of Ni/Mo=1 are amorphous crystals, whereas the sample is completely crystallized at molar ratio of Ni/Mo=2. This behavior implies that the synthesized nanocrystals with an excess of $NiCl_2$ make enhanced nucleation. Figure 1 displays X-ray diffraction patterns of synthesized nanocrystals with molar ratio of Ni/Mo=2 at different pH values. The obtained nanocrystals consist of two phases at pH values less than 10. The first phase is the main phase of 4,4′-Bipyridine-dichloronickel [formula: $C_{10}H_8Cl_2N_2Ni$] related to JCPDS No. 00-050-2049 and the second phase is the smaller phase of Nickel Molybdenum Oxide [formula: $NiMoO_4$] related to JCPDS No. 00-045-0142 (For better resolution, the main phase peaks are indicated with the * sign in Fig. 1 and the rest of the peaks are related to the $NiMoO_4$ phase.). The main phase,

which is orthorhombic at pH values of 4, 6 and 8, shows the three highest peaks at $2\theta \approx 14.785$, $2\theta \approx 10.781$ and $2\theta \approx 24.738$. At pH value of 2, the minor phase is the dominant phase with the first highest peak at $2\theta \approx 26.580$, the second highest peak at $2\theta \approx 27.192$ and the third highest peak at $2\theta \approx 26.552$. The observed small peaks at $2\theta > 35$ are related to diffraction peaks of the minor phase. The existence of this phase shifts the peaks of the major peaks towards higher angles. Therefore, there is a small overlap between the diffraction peaks of these two phases. Increasing the pH value from 2 to 4 and 6 results in significant decrease in peak intensity of minor phase, however, the intensity of main diffraction peaks enhance remarkably. At the pH value of 8, the peak intensities of major phase diminish slightly. Finally, the peak broadening, which occurs at the pH value of 10, indicates the formation of amorphous phase. Therefore, according to these results, the formation of major phase takes place under neutral or low base conditions, while the formation of minor phase occurs under acidic conditions.

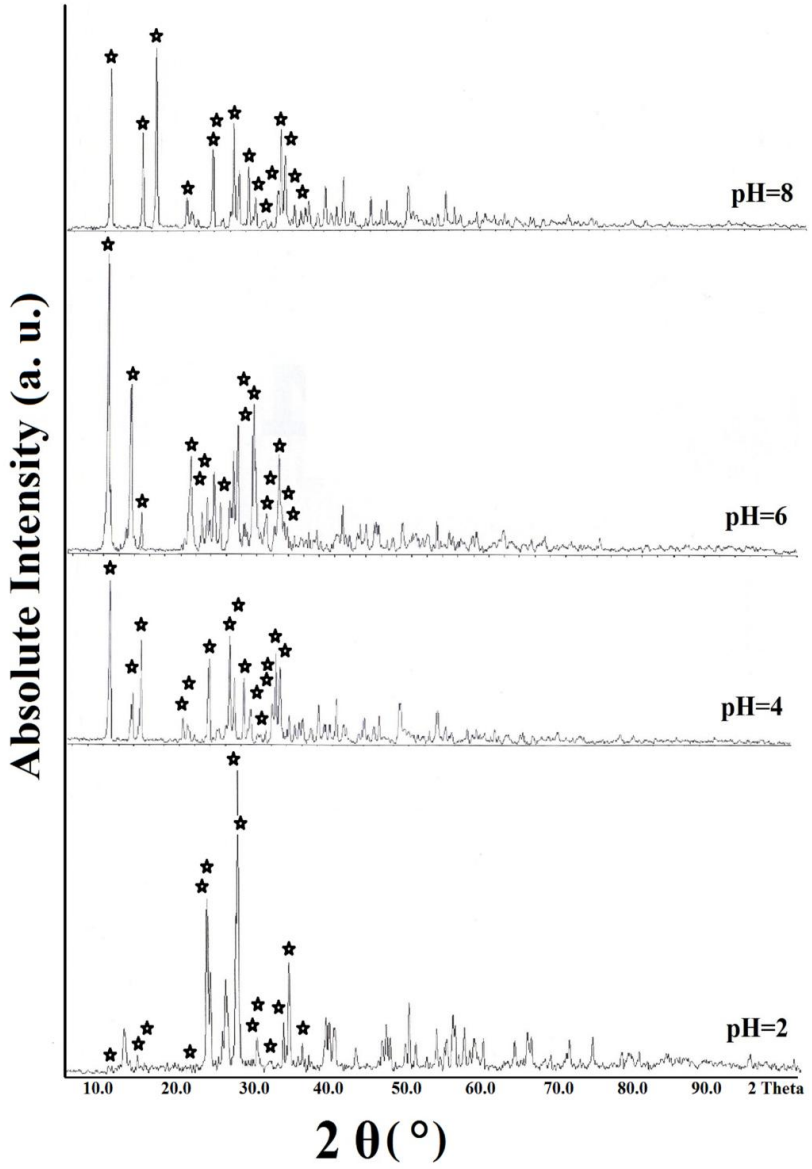

*Figure 1: XRD patterns of synthesized nanocrystals with molar ratio of Ni/Mo=2 at different pH values (the main phase peaks are indicated with the * sign).*

Using scherrer equation, the average crystallite sizes are estimated:

$$D = 0.9\,\lambda / \beta \,\mathrm{Cos}\,\theta$$

Where D is particles size, λ is the CuKα radiation wavelength (λ =1.54060 Å), β is the full width at half maxima (FWHM), θ is the Bragg's diffraction angle. The calculated results of the five highest diffraction peaks at different pH values are listed in table 1. The average crystallite sizes at different pH values are measured in the range of 35-55 nm. Hence, the crystallite sizes show remarkable change upon changing the pH value.

Table 1: The average crystallite sizes of the five highest diffraction peaks at different pH values

Peak No.	$D_{(pH=2)}$(nm)	$D_{(pH=4)}$(nm)	$D_{(pH=6)}$(nm)	$D_{(pH=8)}$(nm)
1	45.15	48.90	52.29	48.82
2	44.78	40.39	44.33	40.88
3	54.53	40.85	44.50	41.38
4	52.07	49.52	48.54	54.31
5	35.56	37.88	40.77	44.13

Scanning electron microscopy

Figure 2 displays the SEM images of those crystals prepared with molar ratio of Ni/Mo=2 at different pH values. The results show that morphology of nanocrystals change at different pH values. Nanocrystals are spherical with the size of 56 nm at the pH values of 6. However, they are planar and lath-like with the sizes of 100-200 nm at the pH values of 2, 4, 8 and 10. Thus, the smallest size of the crystals can be observed at the pH value of 6. The SEM results suggest that morphology of nanostructures is changed with the increment in pH value.

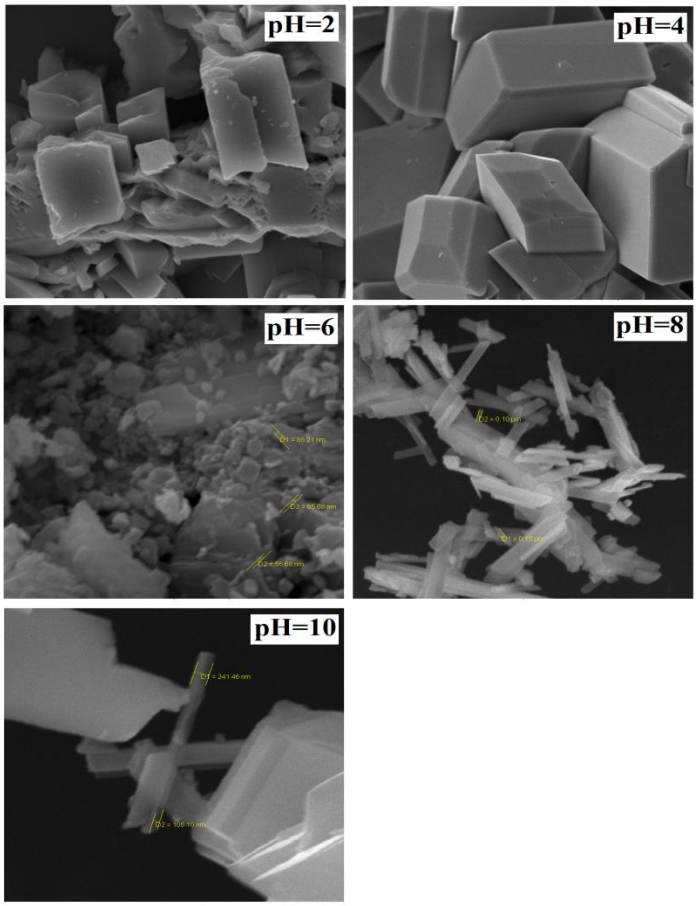

Figure 2: SEM images of nanocrystals prepared with molar ratio of Ni/Mo=2 at different pH values

Energy dispersive X-ray spectroscopy

According to figure 3, EDX elemental analysis of products at the pH values 2-10 confirms the presence of Mo, Ni, and 4,4′-bipy in both major and minor phases. It can be concluded that, The structure of the prepared compound includes 4,4′-bipy spacer groups that MoO_4 units act as bridges among 4,4′-bipy spacer groups and as a result a 3D network with 56 nm in size is formed at neutral pH is form.

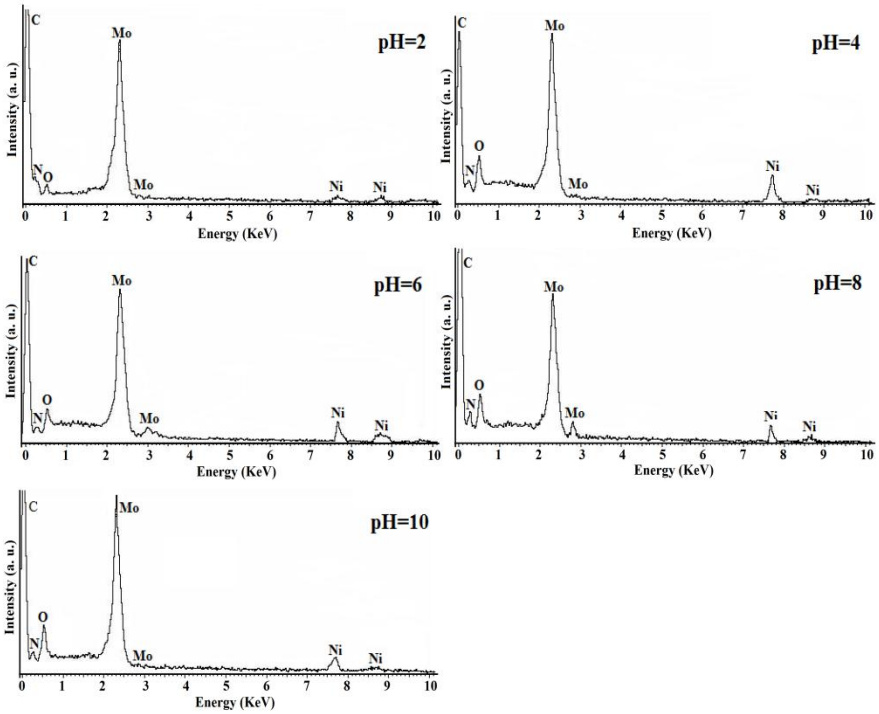

Figure 3: EDX elemental analysis of prepared nanopowders at the pH values 2-10

In Table 2 have been listed the percentages and weight ratios derived from EDX elemental analysis. The results indicate that the ratio of Ni/Mo and Ni/C weight percentages is increased by increasing the pH value. The ratio of Ni to Mo at pH 4 and 6 are approximately 1 to 2.

Table 2: The percentages and weight ratios obtained from EDX elemental analysis of products at pH 2-10

pH	2	4	6	8	10
Mo (Wt %)	38.25	36.37	41.49	30.47	36.32
Ni (Wt %)	10.80	20.08	20.17	22.91	29.49
C (Wt %)	42.60	31.30	31.42	35.05	24.80
N (Wt %)	6.53	2.53	1.54	3.55	2.25
O (Wt %)	1.82	9.72	5.38	8.02	7.14
Ni/Mo	0.28	0.55	0.49	0.75	0.81
Ni/C	0.25	0.64	0.64	0.65	1.19

Fourier transforms infrared spectroscopy

The IR data of prepared products at different pH values in the range of 2-10 are listed in table 3. The stretching vibrations related to Ni-O, Ni-N, O-H, C=N and C=C of 4,4′-bipy ring are observed in the range of 525-573, 641-727, 3374-3524, 1211-1235 and 1605-1612 cm^{-1}, respectively. Furthermore, the symmetric and anti-symmetric stretching vibrations of MoO_2 groups are identified around 802-868 and 892-939 cm^{-1}.

Table 3: IR characteristic bands frequencies (cm^{-1}) of the synthesized compounds at different pH values

Characteristic bands	pH=2	pH=4	pH=6	pH=8	pH=10
$\nu_{(OH)}$	3435.69	3374.06	3524.64	3445.92	3439.03
$\nu_{(C-H)}$	3075.40	2939.53	3142.99	3087.36	2924.70
$\nu_{(C=C)}$	1605.35	1605.46	1605.62	1611.51	1612.39
	1471.68	1509.86	1404.35	1407.95	1488.79
$\nu_{(C=N)}$	1234.55	1229.53	1235.09	1213.53	1211.31
$\nu_{(MoO2)}$	851.44	868.43	802.96	860.34	861.81
	923.22	921.83	892.93	939.18	930.72
$\nu_{(Ni-N)}$	654.06	643.01	672.23	727.45	641.80
$\nu_{(Ni-O)}$	560.41	562.46	573.38	555.57	525.58

Thermogravimetric analysis

Figure 4 indicates the TGA and DTA thermal analysis of optimized nanocrystal at the pH value of 6. The TGA analysis of fabricated product displays two-step weight loss at a heating rate of 5 °C/min in air. The first 6.95%-weight loss at 305-340 °C can be assigned to leaving coordinated water molecules corresponding to the endothermic minimum (330.89 °C) of the DTA curve. The second observed 3.77%-weight loss at 395-455 °C is due to decomposition of 4,4′-bipy ligand and complex structure confirming by the exothermic DTA maximum (429.09 °C). The total weight loss of 10.73 % is in agreement with the calculated data, and so it has thermal resistance.

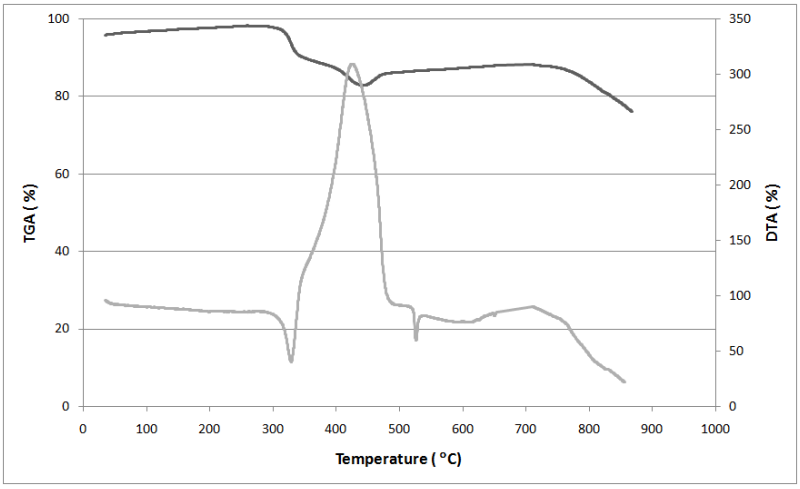

Figure 4: The TGA-DTA thermal analysis of prepared nanocrystal at pH=6

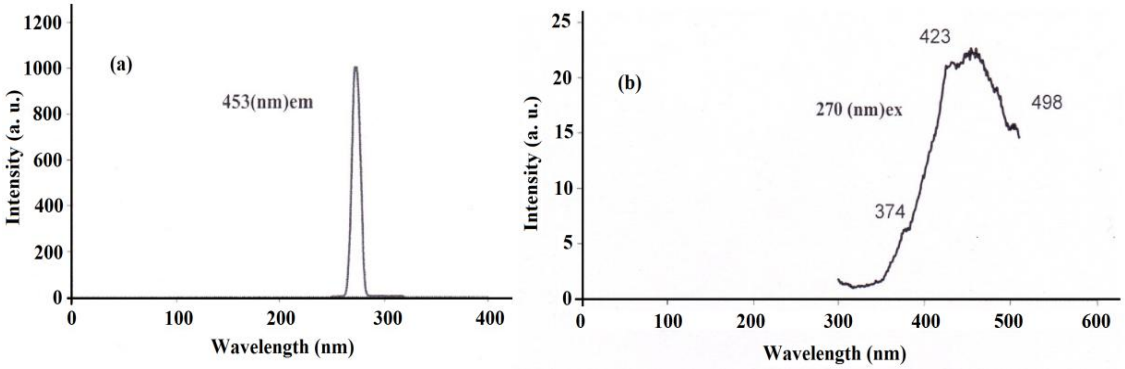

Figure 5: The a) absorbance and b) emission spectra of nanocrystals prepared at pH=6 in solid state at room temperature

Photoluminescence spectra

The absorbance and emission spectra of nanocrystals optimized at the pH value of 6 at room temperature are presented in figure 5. The excited nanocrystals at the wavelength of 270 nm show an intense PL emission peak at the wavelength of 453 nm. This band confirms its optical properties which depend on energy difference between valence and conduction bands. Placement of 4,4′-bipy groups between inorganic materials increases the hardness of structure and leads to observation of photoluminescence emission as a result.

Conclusion

A new inorganic-organic hybrid compound has been synthesized via hydrothermal method using $NiCl_2$, MoO_3 and 4,4′-biyp. This compound shows that interesting multi-dimensional structures can be obtained via covalently linked the inorganic MoO_4 group to complexes of transition metals, such as Ni-biyp. It was observed that molar ratios of Ni/Mo, pH values, temperature and reaction time effectively influence the morphology and nanostructure of final crystals. By fixing different parameters, the crystal sizes increase when the pH value is increased, and particles with size higher than 56 nm are formed. On the basis of obtained results, the crystallization of nanocrystals at the pH value of 6 is optimized and is controlled by a random nucleation process. The results indicate that the ratio of Ni/Mo weight percentages is increased by increasing the pH value.

Using PL spectroscopy, the optical properties of the synthesized samples, originating from the energy difference between conduction and valence bands, are confirmed. Room-temperature PL, which was excited at the wavelength of 270 nm, indicates a photoluminescence emission peak at the wavelength of 453 nm. The fabricated structure displays an increase in hardness as well as a photoluminescence emission due to the fact that 4,4′-biyp groups stand like bridges between inorganic species.

References

1. Samiey, B., Cheng, C-H., Wu, J. (2014). Organic-inorganic hybrid polymers as adsorbents for removal of heavy metal ions from solutions: a review. *Materials, 7*(2):673-726.
2. Yaghi, O.M., OKeeffe, M., Ockwig, N.W., Chae, H.K., Eddaoudi, M., Kim, J. (2003). Reticular synthesis and the design of new materials. *Nature, 423*:705-714.
3. Sanchez, C., Julian, B., Belleville, P., Popall, M. (2005). Applications of hybrid organic–inorganic nanocomposites. *Journal of Materials Chemistry, 15*(35-36):3559-3592.
4. Wang, Y., Yu, J., Du, Y., Shi, Z., Zou, Y., Xu, R. (2002). Hydrothermal synthesis and characterization of a new inorganic–organic hybrid layered zinc phosphate–phosphite $(C_6H_{15}N_2)_2Zn_4(PO_4)_2(HPO_3)_2$. *Journal of the Chemical Society, Dalton Transactions,* (21):4060-4063.
5. Lin, Z.E., Yao, Y.W., Zhang, J., Yang, G.Y. (2002). Synthesis and structure of a novel open-framework zincophosphate with intersecting three-dimensional helical channels. *Journal of the Chemical Society, Dalton Transactions,* (24):4527-4528.
6. Khlobystov, A.N., Blake, A.J., Champness, N.R., Lemenovskii, D.A., Majouga, A.G., Zyk, N.V., Schroder, M. (2001). Supramolecular design of one-dimensional coordination polymers based on silver (I) complexes of aromatic nitrogen-donor ligands. *Coordination Chemistry Reviews, 222*(1):155-192.
7. Madeira, L.M., Portela, M.F., Mazzocchia, C. (2004). Nickel molybdate catalysts and their use in the selective oxidation of hydrocarbons. *Catalysis Reviews, Science and Engineering, 46*(1):53-110.
8. Chang, J.S., Hwang, J.S., Jhung, S.H., Park, S.E., Ferey, G., Cheetham, A.K. (2004) Nanoporous metal-containing nickel phosphates: A class of shape-selective catalyst. *Angewandte Chemie International Edition, 43*(21):2819-2822.
9. Perles, J., Iglesias, M., Martin-Luengo, M.A., Monge, M.A., Ruiz- Valero, C., Snejko, N. (2005). Metal−organic scandium framework: useful material for hydrogen storage and catalysis. *Chemistry of Materials, 17*(23):5837-5842.

10. Kuznicki, S.M., Bell, V.A., Mair, S., Hillhouse, H.W., Jacubinas, R.M., Braunbarth, C.M., Toby, B.H., Tsapatsis, M. (2001). A titanosilicate molecular sieve with adjustable pores for size-selective adsorption of molecules. *Nature (London), 412*(6848):720-724.
11. Clearfield, A. (2000). Inorganic ion exchangers, past, present, and future. *Solvent Extraction and Ion Exchange, 18*(4):655-678.
12. Coronado, E., Galan-Mascaros, J.R., Gimenez-Saiz, C., Gomez-Garcia, C.J., Martinez-Ferrero, E., Almeida, M., Lopes, E.B., Capelli, S.C., Llusar, R.M. (2004). New conducting radical salts based upon Keggin-type polyoxometalates and perylene. *Journal of Materials Chemistry, 14*(12):1867-1872.
13. Coronado, E., Gimenez-Saiz, C., Gomez-Garcia, C.J., Capelli, S.C. (2004). Metallic conductivity down to 2 K in a polyoxometalate-containing radical salt of BEDO-TTF. *Angewandte Chemie International Edition, 43*(23):3022-3025.
14. Shi, Z., Peng, J., Gomez-Garcia, C.J., Benmansour, S., Gu X. (2006). Influence of metal ions on the structures of Keggin polyoxometalate-based solids: Hydrothermal syntheses, crystal structures and magnetic properties. *Journal of Solid State Chemistry, 179*(1):253-265.
15. Clemente-Juan, J.M., Coronado, E. (1999). Magnetic clusters from polyoxometalate complexes. *Coordination Chemistry Reviews, 193-195*:361-394.
16. Nezamzadeh-Ejhieh, A., Salimi, Z. (2010). Heterogeneous photodegradation catalysis of o-phenylenediamine using CuO/X zeolite. *Applied Catalysis A: General, 390*(1-2):110-118.
17. Wang, Q., Tang, H., Xie, Q., Jia, X., Zhang, Y., Tan, L., Yao, S. (2008). The preparation and characterization of poly(o-phenylenediamine)/gold nanoparticles interface for immunoassay by surface plasmon resonance and electrochemistry. *Colloids and Surfaces B: Biointerfaces, 63*(2):254-261.
18. Palys, B., Bokum, A., Rogalski, J. (2007). Poly-o-phenylenediamine as redox mediator for laccase. *Electrochimica Acta, 52*(24):7075-7082.
19. Duan, L.-M., Xu, J.-Q., Xie, F.-T., Cui, X.-B., Ding, H., Song, J.-F. (2005). Synthesis and characterization of a new compound based on mixed Mo/V polyoxometalates connected and modified by $[Ni(en)_2]^{+2}$ groups. *Mendeleev Communications, 15*(2):79-80.
20. Wu, L., Ma, H., Han, Z., Li, C. (2009). Synthesis, structure and property of a new inorganic–organic hybrid compound $[Cu(phen)_2][Cu(phen)H_2O]_2[Mo_5P_2O_{23}].3.5H_2O$. *Solid State Sciences, 11*(1):43-48.
21. Ma, H.-Y., Wu, L.-Z., Pang, H.-J., Meng, X., Peng, J. (2010). Hydrothermal synthesis of two Anderson POM-supported transition metal organic–inorganic compounds. *Journal of Molecular Structure, 967*(1-3):15-19.
22. Niu, J.Y., Guo, D.J., Wang, J.P., Zhao, J.W. (2004). 1D Polyoxometalate-based composite compounds derived from the Wells−Dawson subunit: synthesis and crystal structure of $[\{Ce(DMF)_4(H_2O)_3\}\{Ce(DMF)_4(H_2O)_4\}(P_2W_{18}O_{62})]\cdot H_2O$. *Crystal Growth & Design, 4*(2):241-247.
23. Dolbecq, A., Mialane, P., Lisnard, L., Marrot, J., Secheresse, F. (2003). Hybrid organic–inorganic 1D and 2D frameworks with ε-Keggin polyoxomolybdates as building blocks. *Chemistry - A European Journal, 9*(12):2914-2920.
24. Burkholder, E., Zubieta, J. (2004). A two-dimensional bimetallic oxide constructed from ζ-octamolybdate clusters and Ag(I)-tpyprz cationic polymer components. *Solid State Sciences, 6*(12):1421-1428.
25. Bu, W.-M., Ye, L., Yang, G.-Y., Gao, J.-S., Fan, Y.-G., Shao, M.-C., Xu, J.-Q. (2001). One- and two-dimensional framework materials constructed from the mixed Mo/V tetra-capped Keggin structure clusters and $M(en)_2$ (M=Ni, Cu) complexes groups. *Inorganic Chemistry Communications, 4*(1):1-4.
26. Hagrman, D., Hagrman, P., Zubieta, J. (2000). Polyoxomolybdate clusters and copper–organonitrogen complexes as building blocks for the construction of composite solids. *Inorganica Chimica Acta, 300-302*:212-224.
27. Zhong Lu, C., Wu, C.-De., Zhuang, H.H., Huang, J.S. (2002). Three polymeric frameworks constructed from discrete molybdenum oxide anions and 4,4'-bpy-bridged linear polymeric copper cations. *Chemistry of Materials, 14*(6):2649-2655.

28. Shi, Z., Feng, S.H., Gao, S., Zhang, L.R., Yang, G.Y., Hua, J. (2000). Inorganic–organic hybrid materials constructed from $[(VO_2)(HPO_4)]_\infty$ helical chains and $[M(4,4'\text{-bpy})_2]^{2+}$ (M=Co, Ni) fragments. *Angewandte Chemie International Edition*, *39*(13):2325-2327.
29. Han, G.H., Lin, B.Z., Li, Z., Sun, D.Y., Liu, P.D. (2005). Hydrothermal synthesis and characterization of a new hybrid organic–inorganic compound $[Cd(en)_3]MoO_4$. *Journal of Molecular Structure*, *741*(1):31-35.